Contrast-Enhanced Ultrasound Features of Adult Xp11.2 Translocation Renal Cell Carcinoma

Differential Diagnosis With Three Main Renal Cell Carcinoma Subtypes

Wenliang Ma, MD, Fan Zhang, MD [ID]**, Haifeng Huang, MD, Wei Wang, MD, Yiqi Zhu, MD, Yanwen Lu, MD, Hongqian Guo, MD, Weidong Gan, MD** [ID]

Abbreviations

AUC, area under the curve; ccRCC, clear cell renal cell carcinoma; CEUS, contrast-enhanced ultrasound; chRCC, chromophobe renal cell carcinoma; CI, confidence interval; ICC, interclass correlation coefficient; pRCC, papillary renal cell carcinoma; ROC, receiver operating characteristic; US, ultrasound; Xp11.2 tRCC, Xp11.2 translocation renal cell carcinoma

doi:10.1002/jum.15951

Objectives—To investigate the sonographic features in Xp11.2 translocation renal cell carcinoma (Xp11.2 tRCC) using both conventional ultrasound (US) and contrast-enhanced US (CEUS) and evaluate the usefulness of sonographic imaging characteristics to differentiate between Xp11.2 tRCC and the three common RCC subtypes.

Methods—Thirty-four adult Xp11.2 tRCC patients who preoperatively underwent both conventional US and CEUS and had solitary renal lesions and pathological confirmation after surgery were enrolled. Control matched patients included 131 with clear cell RCC (ccRCC), 48 with papillary RCC (pRCC), and 35 with chromophobe RCC (chRCC). Conventional US and CEUS data of all patients were retrospectively analyzed and compared.

Results—Xp11.2 tRCC was more common in young women. The echogenicity of Xp11.2 tRCC lesions was hypo- and isoechoic relative to the adjacent renal cortex. A higher frequency of calcification within tumors was detected in Xp11.2 tRCC, but the presence of color flow signal (26.5%, 9/34) was much lower. Regarding CEUS features relative to the adjacent renal cortex, synchronous wash-in (61.8%, 21/34), iso-enhancement at peak (55.9%, 19/34), and fast wash-out (50.0%, 17/34) were more common in Xp11.2 tRCC. Moreover, an integrated variables model based on these features could differentiate Xp11.2 tRCC from ccRCC, pRCC, and chRCC (area under the curve, sensitivity, and specificity: 0.934, 92.0%, and 86.0%; 0.907, 88.0%, and 87.0%; and 0.808, 65.0%, and 99.0%, respectively).

Conclusions—Combining conventional US and CEUS lesion features with clinical information may provide a feasible and effective method to differentiate Xp11.2 tRCC from ccRCC, pRCC, and chRCC.

Key Words—contrast-enhanced ultrasound; differential diagnosis; *TFE3*; renal cell carcinoma; Xp11.2 translocation

Renal cell carcinomas (RCCs) are the most common primary malignant kidney tumors. Clear cell renal cell carcinoma (ccRCC), papillary renal cell carcinoma (pRCC), and chromophobe renal cell carcinoma (chRCC) are the common subtypes, accounting for approximately 70%, 15–20%, and 6–11% of all RCCs, respectively.[1–4] Xp11.2

translocation renal cell carcinoma (Xp11.2 tRCC) is a rare subtype of RCC, characterized by a chromosomal translocation involving the transcription factor binding to IGHM enhancer 3 (*TFE3*) gene located on the X chromosome and the nuclear overexpression of *TFE3*.[5] Given that *TFE3* belongs to the microphthalmia-associated transcription factor (MiT) family, Xp11.2 tRCC is classified as a MiT family translocation RCC in the 2016 World Health Organization renal tumor classification scheme.[3] Recent studies have reported that the clinical manifestation of Xp11.2 tRCC in adults is more aggressive than that of ccRCC.[6,7] Due to this aggressive nature and because RCC is generally detected at an advanced stage, adult patients with strongly positive *TFE3* expression tend to have a worse prognosis than those with *TFE3*-negative RCC, that is, ccRCC, pRCC, and chRCC.[8,9] Furthermore, The 2019 European Association of Urology guidelines strongly recommended that clinical stage T1 (T1a or T1b) RCCs should be treated with partial nephrectomy.[10] However, the results from multi-center clinical research showed that stage T1b patients with Xp11.2 tRCC who underwent radical nephrectomy had a more favorable progression-free survival than those who underwent partial nephrectomy.[11] Consequently, an accurate pre-operative diagnosis of Xp11.2 tRCC becomes a critical issue for distinguishing it from other common subtypes of RCCs and designing more appropriate surgical plans.

Multimodality imaging, including conventional ultrasound (US), contrast-enhanced US (CEUS), computed tomography (CT), and multi-parametric magnetic resonance imaging (MRI), is crucial for pre-operative diagnosis and differentiation of renal tumors.[12] Previous studies have reported that CT characteristics and dynamic contrast-enhanced patterns are useful for differentiating Xp11.2 tRCC from ccRCC and pRCC.[13,14] Moreover, multi-parametric MRI characterized Xp11.2 tRCC lesions as mild hyperintensity in T1-weighted imaging, heterogeneous intensity in T2-weighted imaging, and moderate rim enhancement in dynamic contrast-enhanced MRI.[15,16] In contrast, few studies have investigated the imaging features of Xp11.2 tRCC using conventional US and CEUS. US imaging, which is a real-time, non-radioactive, and less nephrotoxic technique, is a valuable additional tool for differentiating renal tumors and has seen rapid developments in recent years, especially for the purpose of differential diagnosis. Previous studies that investigated the characteristics of 22 Xp11.2 tRCC cases using US and CEUS have reported that specific CEUS features may help differentiate Xp11.2 tRCC from ccRCC and pRCC.[17,18] However, these reports had small sample sizes, and they did not evaluate the enhancement patterns and morphological features of Xp11.2 tRCC in detail or assess CEUS usefulness for the differential diagnosis of Xp11.2 tRCC and chRCC.

In this study, we aimed to retrospectively investigate Xp11.2 tRCC lesion features using the conventional US and CEUS for distinguishing this rare subtype from all three main RCC subtypes based on the largest number of pathologically proven positive samples ever reported.[17,18] We hypothesized that these conventional US and CEUS lesion features might prove to be effective tools for differentiating Xp11.2 tRCC from the three main subtypes of RCCs.

Materials and Methods

Patient Selection

The study was approved by the Institutional Review Board of Nanjing Drum Tower Hospital and conducted in accordance with the Declaration of Helsinki; written informed consent was waived due to the retrospective and observational nature of the investigation. We screened consecutive patients with RCC who underwent surgery at Nanjing Drum Tower Hospital between January 2010 and June 2021. Thirty-four adult patients (age range: 22–73 years, mean age: 38.97 ± 13.22 years; 13 men and 21 women) with pathologically proven Xp11.2 tRCC based on both *TFE3* immunohistochemistry and fluorescence in situ hybridization assay were enrolled in our study. These patients preoperatively underwent both CEUS and conventional US examinations to evaluate the renal masses. During the same time period, we searched for patients with pathologically proven ccRCC, pRCC, and chRCC as matched control patients who also underwent preoperative CEUS and conventional US examination. Accordingly, 131 patients with ccRCC (age range: 33–84 years, mean age: 58.89 ± 11.65 years; 96 men and 35 women), 48 with pRCC (age range: 20–86 years, mean age: 57.69 ± 12.55 years; 30 men and 18 women), and 35 with chRCC (age range: 28–83 years, mean age:

49.94 ± 12.56 years; 24 men and 11 women) were included in our study. Overall, 248 patients without other underlying diseases had solitary renal lesions and pathological confirmation after surgery. The clinicopathologic records and diagnostic imaging data of these patients were retrospectively investigated.

Conventional US and CEUS

All patients were examined by the same ultrasonologist with over 15 years of experience in urogenital US imaging. Conventional US was performed using a HITACHI HI VISION Preirus US system with an EUP-C715 probe (frequency range: 3–5 MHz). First, tumor location, diameter, shape, cystic component, echogenicity, and borders were detected using the gray-scale US. Then, color Doppler flow imaging (CDFI) was used to observe blood flow within and outside the renal lesions. Subsequently, CEUS was performed using the same scanning system and probe as the conventional US to continuously observe tissue blood perfusion. During contrast-enhanced imaging, the scanning system contrast mode mechanical index was set at 0.05–0.07. SonoVue (Bracco Imaging, Milan, Italy) mixed with 5 mL of 0.9% saline was used as the contrast agent—2.4 mL of the contrast material was intravenously injected as a bolus, followed by immediate flushing with 5 mL of 0.9% saline. The timer was started as soon as the contrast agent was administered. Patients were instructed to hold their breath or only breathe slowly and shallowly during the imaging process. CEUS videos of the entire process were recorded for at least 3 min for evaluation and interpretation.

Image Interpretation

Videos of both conventional US and CEUS were retrospectively investigated independently by two experienced ultrasonologists who were blinded to the clinicopathologic records and diagnostic imaging data. Any disagreements were resolved by consensus. The characteristics of renal lesions evaluated using conventional US imaging included tumor location, diameter, shape, cystic component, echogenicity, calcification, and blood flow. Renal masses echogenicity was classified as either hyperechoic, isoechoic, or hypoechoic compared to that of the renal cortex. Renal mass features such as wash-in/wash-out, peak enhancement, homogeneity, and presence of pseudocapsule were also reviewed on CEUS imaging.

The wash-in pattern was categorized as fast-in, synchronous-in, or slow-in, and the wash-out pattern as fast-out, synchronous-out, or slow-out as previously described.[19] The peak enhancement included hyper-, iso-, or hypo-enhancement. At peak enhancement, lesions with uniform enhancement were defined as having homogeneous enhancement (homogeneity), and lesions with areas without any enhancement were defined as having heterogeneous enhancement (heterogeneity).[19] The pseudocapsule was defined as the rim of perilesional enhancement after contrast agent injection; the control for the lesions in the enhancement mode was always the adjacent renal cortex.[19]

Statistical Analysis

Statistical analysis was performed using SPSS version 23.0 (SPSS Inc., Chicago, IL, USA) and Stata 12.0 (Stata Corp., Texas, USA). Numeric data are expressed in terms of the mean ± standard deviation and categorical data in percentage. The Student's t-test was used for evaluating numeric data, and the Pearson chi-square (χ^2) test or Fisher's exact test was used for categorical data. Significant variables in univariate logistic analysis were analyzed using multivariate logistic regression analysis to differentiate Xp11.2 tRCC from the three main RCC subtypes. Logistic regression models were established using variables from multivariate logistic regression analysis, and area under the curve (AUC), sensitivity, and specificity were calculated. Inter-observer agreement between the two ultrasonologists was evaluated by calculating interclass correlation coefficients (ICCs). The ICC values were interpreted as follows: ICC < 0.20, poor agreement; ICC = 0.20–0.40, fair agreement; ICC = 0.40–0.75, good agreement; ICC > 0.75 excellent agreement.[19] P-values <.05 were considered statistically significant.

Results

Patients and Tumor Characteristics

The patient and tumors characteristics according to RCC subtypes are shown in Table 1. Of the 34 adult patients with Xp11.2 tRCC, 25 patients were < 45 years, with a male to female ratio of 1:2.57. Thus, Xp11.2 tRCC appeared to be more common in young women; conversely, ccRCC, pRCC, and chRCC affected older men

more frequently. Statistically, there were significant differences in terms of sex and age between patients with Xp11.2 tRCC and ccRCC, Xp11.2 tRCC and pRCC, as well as Xp11.2 tRCC and chRCC ($P < .05$ for all). There were no significant differences between Xp11.2 tRCC and the three main RCC subtypes regarding renal laterality, diameter, or location of lesions ($P > .05$ for all).

Inter-Observer Reliability

The lesion characteristics of Xp11.2 tRCC and the three main RCC subtypes on the conventional US and CEUS imaging were assessed independently by two investigators. Excellent inter-observer reliability was observed in the conventional US characterization and CEUS features between the two investigators (ICC range: 0.644–0.960).

Conventional US and CEUS

The renal lesion features on conventional US and CEUS imaging are listed in Table 2. In conventional US imaging, the echogenicity of Xp11.2 tRCC lesions was either hypoechoic or isoechoic relative to the adjacent renal cortex, while echogenicity in ccRCC was either hypoechoic or hyperechoic ($P = .036$); moreover, the echogenicity of renal lesions differed significantly between the Xp11.2 tRCC and chRCC ($P = .013$). In Xp11.2 tRCC, a higher number of renal lesions (29.4%, 10/34) had

a cystic component than that in chRCC (8.6%, 3/35) ($P = .027$). However, there were no significant differences in cystic component percentage between Xp11.2 tRCC and ccRCC (25.2%, 33/131) ($P > .05$) and between Xp11.2 tRCC and pRCC (18.7%, 9/48) ($P > .05$).

Significant differences in calcification within renal lesions were observed between Xp11.2 tRCC and the three common RCC subtypes ($P < .001$ for all), and a higher frequency of calcification within tumors was detected in Xp11.2 tRCC. Regarding CDFI, there was a significant difference between Xp11.2 tRCC and ccRCC in the presence of color flow signal, which was much lower in Xp11.2 tRCC lesions (26.5%, 9/34) than in ccRCC (85.5%, 112/131) ($P < .001$).

Based on the wash-in enhancement patterns in CEUS imaging, the arrival time of the contrast agent in 21 of the 34 (61.8%) Xp11.2 tRCC lesions was the same as that in the adjacent renal cortex (Figure 1). A higher percentage (90.1%, 118/131) of synchronous wash-in was observed in ccRCC lesions (Figure 2), but a slow wash-in pattern was observed in pRCC lesions (62.5%, 30/48). Consequently, there were significant differences in the wash-in enhancement patterns between Xp11.2 tRCC and pRCC ($P < .05$, Figure 3). In terms of peak enhancement, the enhancement in the lesions was the same as that in the adjacent renal cortex in 55.9% of patients

Table 1. Patient and General Lesion Characteristics Corresponding to the Four RCC Subtypes

Characteristic	Xp11.2 tRCC N = 34	ccRCC N = 131	pRCC N = 48	chRCC N = 35	P value a*	b**	c***
Age, years	38.97 ± 13.22	58.89 ± 11.65	57.69 ± 12.55	49.94 ± 12.56	<.001	<.001	.001
Sex (%)					<.001	.030	.012
Male	13 (38.2)	96 (73.3)	30 (62.5)	24 (68.6)			
Female	21 (61.8)	35 (26.7)	18 (37.5)	11 (31.4)			
Lesion diameter, cm	4.81 ± 2.25	4.86 ± 1.96	4.21 ± 3.18	4.31 ± 2.32	.901	.346	.359
Laterality (%)					.343	.108	.071
Left	21 (61.8)	69 (52.7)	21 (43.8)	14 (40)			
Right	13 (38.2)	62 (47.3)	27 (56.2)	21 (60)			
Location (%)					.388	.153	.061
Upper	8 (23.5)	47 (35.9)	15 (31.3)	10 (28.6)			
Middle	14 (41.2)	47 (35.9)	25 (52.1)	21 (60)			
Lower	12 (35.3)	37 (28.2)	8 (16.7)	4 (11.4)			

Xp11.2 tRCC, Xp11.2 translocation renal cell carcinoma; ccRCC, clear cell renal cell carcinoma; pRCC, papillary renal cell carcinoma; chRCC, chromophobe renal cell carcinoma.
*Xp11.2 tRCC versus ccRCC.
**Xp11.2 tRCC versus pRCC.
***Xp11.2 tRCC versus chRCC.

Table 2. Conventional US and CEUS features in renal lesions corresponding to the four RCC subtypes

Characteristic	Xp11.2 tRCC N = 34	ccRCC N = 131	pRCC N = 48	chRCC N = 35	P value a*	b**	c***
Echogenicity (%)					.036	.412	.013
Hypo-echoic	14 (41.2)	44 (33.6)	21 (43.8)	15 (42.9)			
Iso-echoic	12 (35.3)	26 (19.8)	11 (22.9)	3 (8.6)			
Hyper-echoic	8 (23.5)	61 (46.6)	16 (33.3)	17 (48.5)			
Cystic component (%)					.617	.260	.027
Absent	24 (70.6)	98 (74.8)	39 (81.3)	32 (91.4)			
Present	10 (29.4)	33 (25.2)	9 (18.7)	3 (8.6)			
Calcification (%)					<.001	<.001	<.001
Present	14 (41.2)	16 (12.2)	2 (4.2)	2 (5.7)			
Absent	20 (58.8)	115 (87.8)	46 (95.8)	33 (94.3)			
Color flow signal (%)					<.001	.281	.110
Present	9 (26.5)	112 (85.5)	8 (16.7)	4 (11.4)			
Absent	25 (73.5)	19 (14.5)	40 (83.3)	31 (88.6)			
Wash-in (%)					<.001	.015	.054
Slow-in	11 (32.4)	7 (5.3)	30 (62.5)	21 (60)			
Synchronous-in	21 (61.8)	118 (90.1)	17 (35.4)	13 (37.1)			
Fast-in	2 (5.8)	6 (4.6)	1 (2.1)	1 (2.9)			
Peak enhancement (%)					<.001	.002	.063
Hypo-enhancement	9 (26.5)	9 (6.9)	30 (62.5)	17 (48.6)			
Iso-enhancement	19 (55.9)	34 (25.9)	10 (20.8)	10 (28.6)			
Hyper-enhancement	6 (17.6)	88 (67.2)	8 (16.7)	8 (22.8)			
Homogeneity (%)					.371	.560	.733
Homogeneity	12 (35.3)	36 (27.5)	20 (41.7)	11 (31.4)			
Heterogeneity	22 (64.7)	95 (72.5)	28 (58.3)	24 (68.6)			
Wash-out (%)					.002	.011	.053
Slow-out	5 (14.7)	53 (40.4)	3 (6.3)	5 (14.3)			
Synchronous-out	12 (35.3)	17 (13.0)	6 (12.5)	4 (11.4)			
Fast-out	17 (50.0)	61 (46.6)	39 (81.2)	26 (74.3)			
Pseudocapsule (%)					<.001	.773	.256
Present	11 (32.4)	89 (67.9)	17 (35.4)	16 (45.7)			
Absent	23 (67.6)	42 (32.1)	31 (64.6)	19 (54.3)			

Xp11.2 tRCC: Xp11.2 translocation renal cell carcinoma; ccRCC, clear cell renal cell carcinoma; pRCC, papillary renal cell carcinoma; chRCC, chromophobe renal cell carcinoma.
*Xp11.2 tRCC versus ccRCC.
**Xp11.2 tRCC versus pRCC.
***Xp11.2 tRCC versus chRCC.

(19/34) with Xp11.2 tRCC. The peak enhancement was hyper-enhanced compared to that in the adjacent renal cortex in 67.2% of patients (88/131) with ccRCC, while hypo-enhancement was more common in pRCC patients (62.5%, 30/48). Moreover, the observed differences in peak enhancement between Xp11.2 tRCC and ccRCC (P < .001) and between Xp11.2 tRCC and pRCC (P = .002) were statistically significant. With respect to the wash-out enhancement patterns, the contrast agent flowed out of the lesions faster than it did from the renal cortex in 50% of Xp11.2 tRCC patients (17/34). Although the fast

wash-out pattern was also more common in ccRCC (46.6%, 61/131) and pRCC (81.5%, 39/48), significant differences were found in the wash-out enhancement patterns between Xp11.2 tRCC and both ccRCC and pRCC (P < .05 for both, Figures 2 and 3). Xp11.2 tRCC and the three common RCC subtypes mainly showed heterogeneous peak enhancement (P > .05), and a higher percentage of pseudocapsules was observed in ccRCC (67.9%, 89/131) than in Xp11.2 tRCC (32.4%, 11/34) (P < .001). Nonetheless, there were no significant differences between Xp11.2 tRCC and chRCC regarding the wash-in, wash-out,

Figure 1. Xp11.2 tRCC in a 42-year-old woman. **A**, hyperechoic lesion located in the lower pole of the left kidney detected using conventional US (arrow). **B**, CDFI shows that the lesion lacks a blood flow signal (arrow). **C**, CEUS shows that enhancement of the lesion is synchronous with that of the renal cortex (arrow). **D**, The lesion shows homogeneous hypo-enhancement at peak (arrow). **E**, The lesion shows fast wash-out in the medullary phase (arrow).
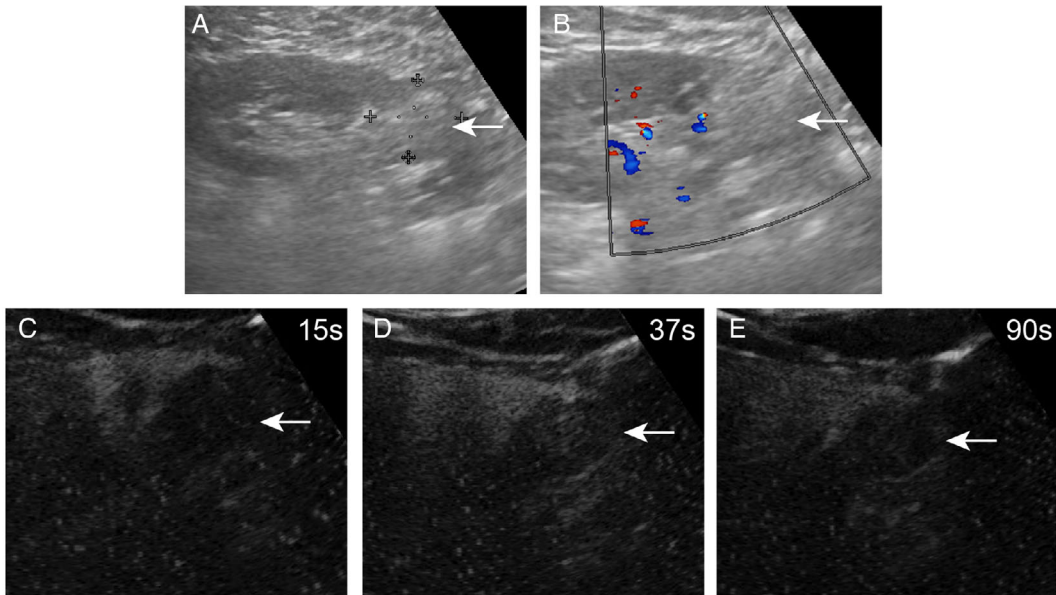

Figure 2. ccRCC in a 55-year-old man. **A**, The isoechoic lesion located in the middle of the left kidney detected using conventional US (arrow). **B**, CDFI shows that the lesion has rich blood flow signaling (arrow). **C**, CEUS shows that the enhancement in the lesion is synchronous with that in the renal cortex (arrow). **D**, The lesion shows heterogeneous hyper-enhancement at peak (arrow). **E**, The lesion shows slow wash-out in the medullary phase (arrow).
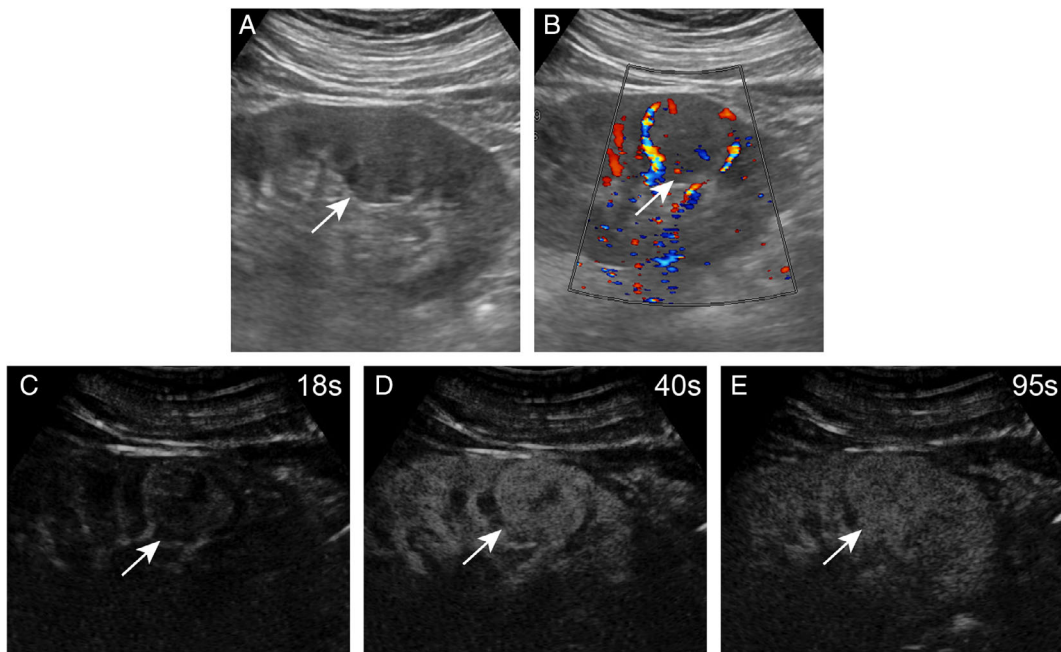
Figure 3. pRCC in a 62-year-old man. **A**, The hypoechoic lesion located in the middle of the left kidney detected using conventional US (arrow). **B**, CDFI shows that the lesion lacks a blood flow signal (arrow). **C**, CEUS shows that the enhancement in the lesion is slower than that in the renal cortex (arrow). **D**, The lesion shows heterogeneous hypo-enhancement at peak (arrow). **E**, The lesion shows fast wash-out in the medullary phase (arrow).
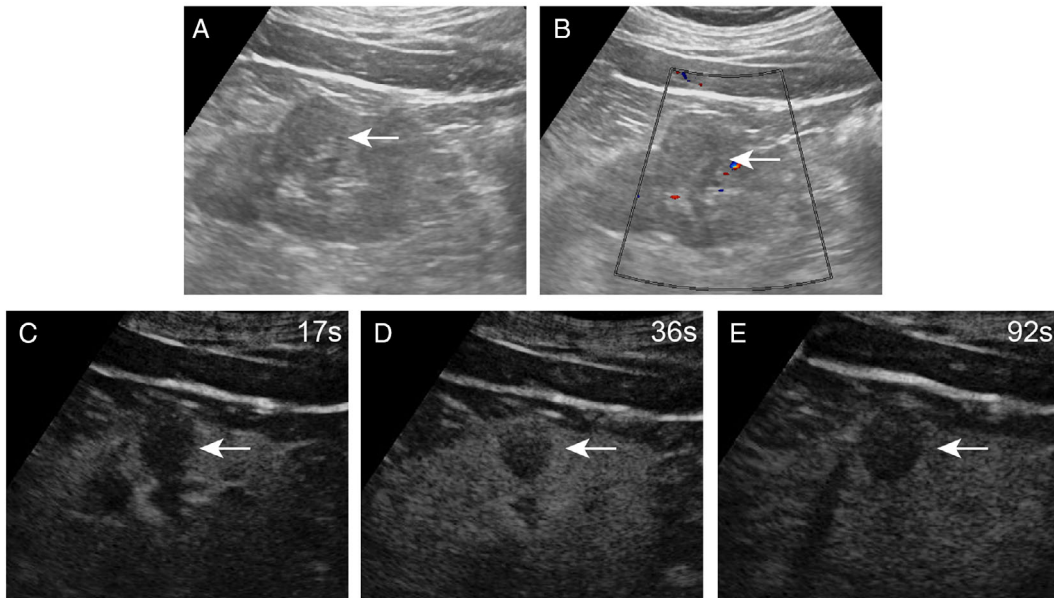
pseudocapsule, or peak enhancement CEUS features ($P > .05$ for all, Figure 4).

### Multivariate Logistic Regression Analysis and Receiver-Operating Characteristic Analysis

Using multivariate logistic regression analysis to differentiate between Xp11.2 tRCC and the three main RCC subtypes, we confirmed that age, sex, and color flow signal were significant predictors for distinguishing Xp11.2 tRCC from ccRCC (all $P < .05$); furthermore, age, wash-out pattern, and calcification were significant predictive factors for differentiating Xp11.2 tRCC from pRCC (all $P < .05$). Finally, age and calcification were the two significant predictors for differentiating Xp11.2 tRCC from chRCC (all $P < .05$; Figure 5A, C, and E). These significant predictive factors were used to construct logistic regression models and obtain receiver-operating characteristic (ROC) curves (Table 3). The ROC curves of the integrated variables models for differentiating Xp11.2 tRCC from ccRCC (sensitivity, 92.0%; specificity, 86.0%; AUC, 0.934), pRCC (sensitivity, 88.0%; specificity, 87.0%; AUC, 0.907), and chRCC

(sensitivity, 65%; specificity, 99%; AUC, 0.808) are shown in Figure 5B, D, and F, respectively.

Discussion

The use of both conventional US and CEUS for evaluating Xp11.2 tRCC is still in the preliminary stages, and few studies have discussed strategies for the differentiation of Xp11.2 tRCC from the common RCC subtypes. With the advances in diagnostic technology and increasing knowledge about the disease, the number of adult patients diagnosed with Xp11.2 tRCC has also increased. CEUS imaging has been shown to be a sensitive technique for differentiating among the RCC subtypes.[17,20,21] The age of onset varies among the different RCC subtypes, as do the male-to-female ratios. The majority of patients with the common RCCs are men. One study on 749 patients (male to female ratio, 1:0.48) reported the mean age of ccRCC diagnosis of 55 years, while another study on 626 patients (male to female ratio, 1:0.28) reported the mean age of pRCC diagnosis of approximately 62 years.[4,22] Similarly, a study on 291 patients showed

Figure 4. chRCC in a 62-year-old woman. **A**, The hypoechoic lesion located in the middle of the left kidney detected using conventional US (arrow). **B**, CDFI shows that the lesion lacks a blood flow signal (arrow). **C**, CEUS shows that the enhancement in the lesion is slower than that in the renal cortex (arrow). **D**, The lesion shows homogeneous hypo-enhancement at peak (arrow). **E**, The lesion shows fast wash-out in the medullary phase (arrow).
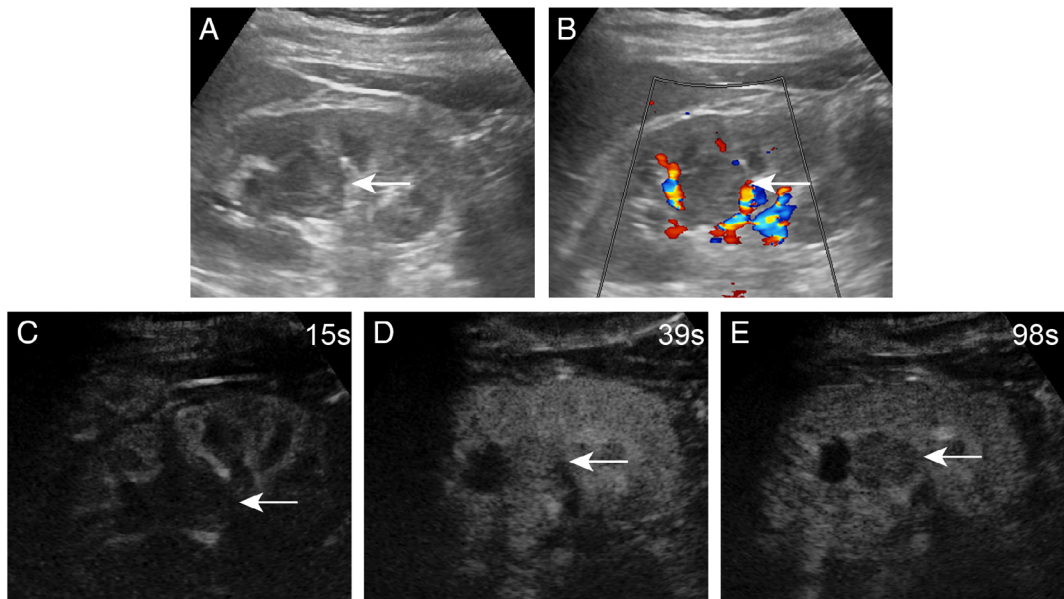
that the mean age in a population of patients with chRCC was 59.9 years and that sex was significantly associated with incidence and prognosis.[1] In contrast, Xp11.2 tRCC is a rare subtype of RCC that occurs predominantly in children and young women.[23,24] Our study also found that the number of female patients was significantly higher than that of males and that the majority of them were aged <45 years, which is a critical factor for identifying Xp11.2 tRCC.

Although it is difficult to differentiate between different RCC subtypes using the conventional US, it is useful to identify Xp11.2 tRCC. Ling et al reported that hyperechoic mixed tumors in the kidney with sharp margins and the presence of calcification were the main features of Xp11.2 tRCC, while Wei et al considered the presence of calcification as the most important feature of Xp11.2 tRCC on conventional US imaging.[17,18] In line with our findings, Xp11.2 tRCC lesions had a higher calcification percentage than common RCC subtype lesions did. Although irregular punctate calcification was more common in Xp11.2 tRCC, wall calcification was also detected in some cases. However, the three main RCC subtypes showed less calcification on conventional US imaging,

although punctate or coarse calcifications were also observed in some cases. Accordingly, the presence of calcification can be considered a predictor for differentiating Xp11.2 tRCC from the three common RCC subtypes. Previous studies on CT features of Xp11.2 tRCC have also confirmed that the renal lesions show circular or rim calcifications, which may be helpful for clinicians in diagnosing Xp11.2 tRCC.[13,14] One study reported that the formation of calcifications might be related to psammoma bodies in the renal lesions,[25] but the exact molecular mechanisms for calcification being more common in Xp11.2 tRCC are unclear. Additionally, the absence of color flow signals in renal lesions was confirmed on conventional US imaging, but peak enhancement on CEUS imaging in 55.9% of patients with Xp11.2 tRCC was iso-enhancement in our study. The absence of color Doppler flow signal in a lesion could indicate that it may be a hypovascular or hemorrhagic cyst. Moreover, CEUS is more sensitive than the conventional US detecting blood vessels. In our study, three cases of Xp11.2 tRCC showed a huge hemorrhagic cyst and absence of color flow signals. In a recent report, patients with Xp11.2 tRCC were found to have a hypervascular

Figure 5. Differentiation of Xp11.2 tRCC from the common RCC subtypes using multivariate logistic regression analysis and ROC curves of the corresponding logistic regression variables. Statistical results of multivariate logistic regression analysis are depicted using forest plots: **A**, Xp11.2 tRCC versus ccRCC. **C**, Xp11.2 tRCC versus pRCC. **E**, Xp11.2 tRCC versus chRCC. ROC curves of the logistic regression variables for differentiating Xp11.2 tRCC from ccRCC (**B**), pRCC (**D**), and chRCC (**F**). CI, confidence interval; OR, odds ratio; ROC, receiver operating characteristic; Xp11.2 tRCC, Xp11.2 translocation renal cell carcinoma; ccRCC, clear cell renal cell carcinoma; pRCC, papillary renal cell carcinoma; chRCC, chromophobe renal cell carcinoma.
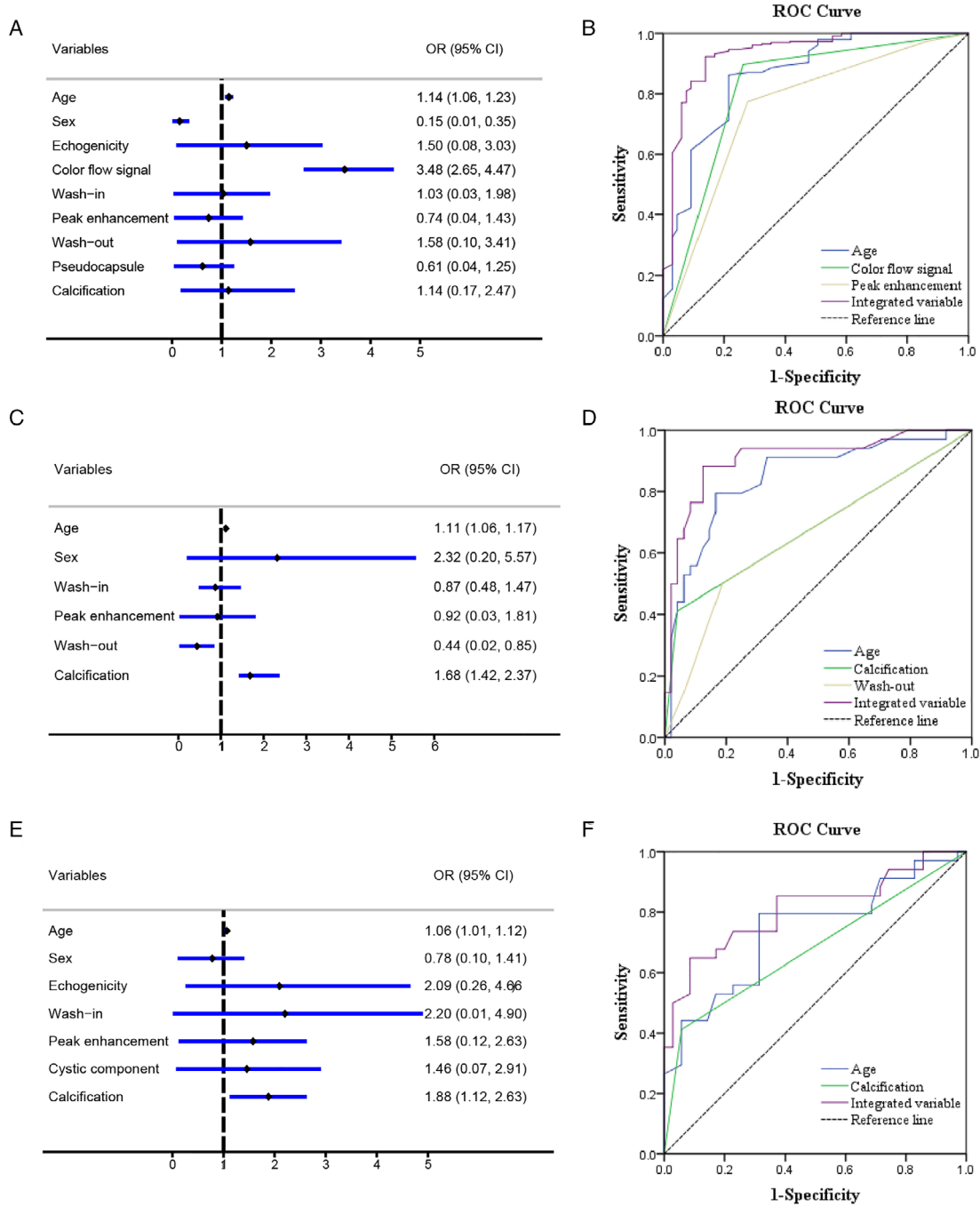
Table 3. Diagnostic performance of logistic regression model variables in differentiating Xp11.2 tRCC from the three common RCC subtypes

Classification	AUC (95% CI)	Sensitivity (%)	Specificity (%)
Xp11.2 tRCC versus ccRCC			
Age	0.860 (0.807–0.914)	86	78
Color flow signal	0.818 (0.752–0.884)	90	74
Peak enhancement	0.755 (0.686–0.823)	77	72
Integrated variables	0.934 (0.897–0.971)	92	86
Xp11.2 tRCC versus pRCC			
Age	0.846 (0.756–0.935)	79	83
Calcification	0.685 (0.562–0.808)	41	99
Wash-out	0.654 (0.531–0.778)	50	81
Integrated variables	0.907 (0.837–0.978)	88	87
Xp11.2 tRCC versus chRCC			
Age	0.737 (0.618–0.856)	79	69
Calcification	0.677 (0.549–0.806)	41	99
Integrated variables	0.808 (0.703–0.913)	65	99

Xp11.2 tRCC, Xp11.2 translocation renal cell carcinoma; ccRCC, clear cell renal cell carcinoma; pRCC, papillary renal cell carcinoma; chRCC, chromophobe renal cell carcinoma; AUC, area under the curve; CI, confidence interval.

lesion with high microvessel density,[26] whereas Xp11.2 tRCC lesions showed a lower degree of enhancement than the normal renal cortex did in contrast-enhanced studies.[27,28] A possible explanation for these varied results is that genomic heterogeneity in Xp11.2 tRCC leads to histological heterogeneity.[29] The microvessel density in Xp11.2 tRCC also varies greatly, as does the microvessel area. The results could also differ because of the differences in sample size between studies. Finally, the results of ultrasound examinations are also affected by subjective factors such as the Doppler gain setting.

Regarding patterns of enhancement, synchronous wash-in, iso-enhancement at peak, and fast wash-out were the main features of Xp11.2 tRCC in our study, and differed completely from those in ccRCC, pRCC, and chRCC. The enhancement patterns in ccRCC reported in previous studies are synchronous wash-in, hyper-enhancement at peak, and fast wash-out, while those in pRCC are of slow wash-in, hypo-enhancement at peak, and fast wash-out,[19,30,31] which are consistent with our findings. Previous studies have also shown that the mean microvessel density is significantly high in ccRCC, but significantly low in pRCC.[26,30] CEUS findings for chRCC were more often characterized by synchronous wash-in, hypo-enhancement at peak, and fast wash-out, although we had speculated that the wash-in pattern in chRCC lesions would be slower than that in the renal cortex.

Investigation of angiogenesis in renal lesions is still critical to understanding these differences in wash-in enhancement patterns. Similar to that in ccRCC, pRCC, or chRCC,[21,31,32] a high percentage of heterogeneous enhancement was observed at peak enhancement in Xp11.2 tRCC lesions. Xp11.2 tRCC often presents with a low percentage of lesions with pseudocapsules, while the presence of pseudocapsules is more common in ccRCC. A previous study reported that the incidence of pseudocapsule in ccRCC was significantly higher in tumors with a diameter within the 2.1–5 cm range,[33] but the association between the presence of pseudocapsule and lesion size in Xp11.2 tRCC warrants further investigation.

To obtain more valuable features for differentiating between Xp11.2 tRCC and the three main RCC subtypes, we performed multivariate logistic regression analysis and ROC analysis. The results suggest that young age, female sex, and absence of color flow signals were significant predictive factors for distinguishing Xp11.2 tRCC from ccRCC. As reported in the literature, ccRCC lesions are hypervascular with high microvessel density, occur more often in older men, and are characterized by simultaneous wash-in, hyper-enhancement at peak, faster wash-out pattern, presence of pseudocapsule, and heterogeneous enhancement at peak on CEUS imaging.[19,26] Although the parameter of peak enhancement was

not regarded as a significant predictor in multivariate logistic regression analysis, it is still valuable for the differentiation of Xp11.2 tRCC and ccRCC. Consistent with our findings, Wei et al explored the differentiation between Xp11.2 tRCC and ccRCC using CEUS and found that lower peak enhancement was more likely to occur in Xp11.2 tRCC than in ccRCC.[17] Nevertheless, pRCC tumors are the most common hypovascular renal tumors and also affect older men.[4,34] Because the histomorphological and radiological findings of Xp11.2 tRCC are extremely similar to those of pRCC;[28] it is difficult to differentiate between Xp11.2 tRCC and pRCC. In this study, multivariate logistic regression analysis identified three predictive factors for differential diagnosis— age, wash-out pattern, and calcification, and an integrated variables model based on these three predictive factors exhibited excellent performance in distinguishing Xp11.2 tRCC from pRCC. Similarly, chRCC commonly occurs in the older male population (mean age, approximately 60 years) and is typically characterized by hypovascular lesions on contrast-enhanced CT.[1,34,35] Conversely, Xp11.2 tRCC mainly occurred in a younger population and showed a higher percentage of calcification on conventional US imaging compared with that in chRCC.[35] While no difference was found in the enhancement patterns between Xp11.2 tRCC and chRCC, a logistic regression model with age and calcification performed well in differentiating Xp11.2 tRCC from chRCC.

This study provided some novel findings; however, it had certain limitations. First, quantitative CEUS imaging analysis may be more useful for differentiating Xp11.2 tRCC from other RCC subtypes. Second, renal cancer includes renal oncocytoma and angiomyolipoma; the enhancement features of their lesions should also be clarified for better differential diagnosis of Xp11.2 tRCC. Third, the sample size of this retrospective study was still relatively small. Finally, the combination of CEUS and contrast-enhanced CT features can provide additional valuable information regarding the differentiation of Xp11.2 tRCC from other RCC subtypes.

Overall, we have confirmed that young age, female sex, and the presence of solid hypo- and isoechoic renal lesions with calcification and low color flow signal on conventional US imaging are useful indicators for diagnosing Xp11.2 tRCC. Moreover, synchronous wash-in, heterogeneous iso-enhancement at peak, and fast wash-out on CEUS images are other useful identifiers. Furthermore, young age and absence of color flow signals combined with lower peak enhancement are more common in Xp11.2 tRCC than in ccRCC. Similarly, young age and the presence of calcification combined with slower wash-out are more likely to be the imaging features of Xp11.2 tRCC than pRCC. Additionally, young age and the presence of calcification had good diagnostic performance in the differential diagnosis of Xp11.2 tRCC and chRCC. Combining conventional US and CEUS lesion characteristics with clinical data may provide a good method to differentiate Xp11.2 tRCC from ccRCC, pRCC, and chRCC.

References

1. Volpe A, Novara G, Antonelli A, et al. Chromophobe renal cell carcinoma (RCC): oncological outcomes and prognostic factors in a large multicentre series. *BJU Int* 2012; 110:76–83. https://doi.org/10.1111/j.1464-410X.2011.10690.x.

2. Tsui KH, Shvarts O, Smith RB, Figlin RA, de Kernion JB, Belldegrun A. Prognostic indicators for renal cell carcinoma: a multivariate analysis of 643 patients using the revised 1997 TNM staging criteria. *J Urol* 2000; 163:1090–1095; quiz 1295. https://doi.org/10.1016/s0022-5347(05)67699-9.

3. Moch H, Cubilla AL, Humphrey PA, Reuter VE, Ulbright TM. The 2016 WHO classification of Tumours of the urinary system and male genital organs-part a: renal, penile, and testicular tumours. *Eur Urol* 2016; 70:93–105. https://doi.org/10.1016/j.eururo.2016.02.029.

4. Ledezma RA, Negron E, Paner GP, et al. Clinically localized type 1 and 2 papillary renal cell carcinomas have similar survival outcomes following surgery. *World J Urol* 2016; 34:687–693. https://doi.org/10.1007/s00345-015-1692-3.

5. Lopez-Beltran A, Scarpelli M, Montironi R, Kirkali Z. 2004 WHO classification of the renal tumors of the adults. *Eur Urol* 2006; 49:798–805. https://doi.org/10.1016/j.eururo.2005.11.035.

6. Gandhi JS, Malik F, Amin MB, Argani P, Bahrami A. MiT family translocation renal cell carcinomas: a 15th anniversary update. *Histol Histopathol* 2020; 35:125–136. https://doi.org/10.14670/hh-18-159.

7. Classe M, Malouf GG, Su X, et al. Incidence, clinicopathological features and fusion transcript landscape of translocation renal cell carcinomas. *Histopathology* 2017; 70:1089–1097. https://doi.org/10.1111/his.13167.

8. Mir MC, Trilla E, de Torres IM, et al. Altered transcription factor E3 expression in unclassified adult renal cell carcinoma indicates adverse pathological features and poor outcome. *BJU Int* 2011; 108:E71–E76. https://doi.org/10.1111/j.1464-410X.2010.09818.x.

9. Qu Y, Gu C, Wang H, et al. Diagnosis of adults Xp11.2 translocation renal cell carcinoma by immunohistochemistry and FISH assays: clinicopathological data from ethnic Chinese population. *Sci Rep* 2016; 6:21677. https://doi.org/10.1038/srep21677.

10. Ljungberg B, Albiges L, Abu-Ghanem Y, et al. European Association of Urology Guidelines on renal cell carcinoma: the 2019 update. *Eur Urol* 2019; 75:799–810. https://doi.org/10.1016/j.eururo.2019.02.011.

11. Liu N, Qu F, Shi Q, et al. Nephron-sparing surgery for adult Xp11.2 translocation renal cell carcinoma at clinical T1 stage: a multicenter study in China. *Ann Surg Oncol* 2021; 28:1238–1246. https://doi.org/10.1245/s10434-020-08813-y.

12. Tsili AC, Andriotis E, Gkeli MG, et al. The role of imaging in the management of renal masses. *Eur J Radiol* 2021; 141:1–14. https://doi.org/10.1016/j.ejrad.2021.109777.

13. He J, Gan W, Liu S, et al. Dynamic computed tomographic features of adult renal cell carcinoma associated with Xp11.2 translocation/TFE3 gene fusions: comparison with clear cell renal cell carcinoma. *J Comput Assist Tomogr* 2015; 39:730–736. https://doi.org/10.1097/rct.0000000000000263.

14. He J, Zhou K, Zhu B, et al. Dynamic contrast-enhanced CT characterization of Xp11.2 translocation/TFE3 gene fusions versus papillary renal cell carcinomas. *Biomed Res Int* 2015; 2015:298679. https://doi.org/10.1155/2015/298679.

15. Liu K, Xie P, Peng W, Zhou Z. Renal carcinomas associated with Xp11.2 translocations/TFE3 gene fusions: findings on MRI and computed tomography imaging. *J Magn Reson Imaging* 2014; 40:440–447. https://doi.org/10.1002/jmri.24349.

16. Wang W, Ding J, Li Y, et al. Magnetic resonance imaging and computed tomography characteristics of renal cell carcinoma associated with Xp11.2 translocation/TFE3 gene fusion. *PLoS One* 2014; 9:e99990. https://doi.org/10.1371/journal.pone.0099990.

17. Wei S, Tian F, Xia Q, et al. Contrast-enhanced ultrasound findings of adult renal cell carcinoma associated with Xp11.2 translocation/TFE3 gene fusion: comparison with clear cell renal cell carcinoma and papillary renal cell carcinoma. *Cancer Imaging* 2019; 20:1–10. https://doi.org/10.1186/s40644-019-0268-7.

18. Ling W, Ma X, Luo Y, et al. Ultrasonographic findings of renal cell carcinomas associated with Xp11.2 translocation/TFE3 gene fusion. *Contrast Media Mol Imaging* 2017; 2017:2958357. https://doi.org/10.1155/2017/2958357.

19. Xue L-Y, Lu Q, Huang B-J, et al. Papillary renal cell carcinoma and clear cell renal cell carcinoma: differentiation of distinct histological types with contrast - enhanced ultrasonography. *Eur J Radiol* 2015; 84:1849–1856. https://doi.org/10.1016/j.ejrad.2015.06.017.

20. Li C, Huang B, Lu Q, et al. The value of contrast-enhanced ultrasound in the differentiation of renal oncocytoma and chromophobe renal cell carcinoma. *Chin J Ultrasonogr* 2020; 29:684–689.

21. Hu R, Zhu T, Che X, Wu L, Tang J. The value of contrast-enhanced ultrasonography in the differential diagnosis of Hypovascular renal cell carcinoma with different pathology subtypes. *Chinese J Ultrasonic Med* 2020; 36:703–706.

22. Chen SH, Xu LY, Wu YP, et al. Tumor volume: a new prognostic factor of oncological outcome of localized clear cell renal cell carcinoma. *BMC Cancer* 2021; 21:79. https://doi.org/10.1186/s12885-021-07795-8.

23. Zhuang W, Liu N, Guo H, Zhang C, Gan W. Gender difference analysis of Xp11.2 translocation renal cell carcinomas's attack rate: a meta-analysis and systematic review. *BMC Urol* 2020; 20:130. https://doi.org/10.1186/s12894-020-00696-1.

24. Cheng X, Gan W, Zhang G, Li X, Guo H. Clinical characteristics of XP11.2 translocation/TFE3 gene fusion renal cell carcinoma: a systematic review and meta-analysis of observational studies. *BMC Urol* 2016; 16:40. https://doi.org/10.1186/s12894-016-0154-6.

25. Liu N, Qu F, Wei K, et al. Incidence and significance of psammoma bodies in Xp11.2 translocation renal cell carcinoma and papillary renal cell carcinoma. *Oncol Lett* 2019; 18:472–478. https://doi.org/10.3892/ol.2019.10305.

26. Ma W, Yang J, Liu N, et al. Are tumor-associated microangiogenesis and lymphangiogenesis considered as the novel prognostic factors for patients with Xp11.2 translocation renal cell carcinoma? *BMC Cancer* 2020; 20:1182. https://doi.org/10.1186/s12885-020-07696-2.

27. Zhu QQ, Wang ZQ, Zhu WR, Chen WX, Wu JT. The multislice CT findings of renal carcinoma associated with XP11.2 translocation/TFE gene fusion and collecting duct carcinoma. *Acta Radiol* 2013; 54:355–362. https://doi.org/10.1258/ar.2012.120255.

28. Kato H, Kanematsu M, Yokoi S, et al. Renal cell carcinoma associated with Xp11.2 translocation/TFE3 gene fusion: radiological findings mimicking papillary subtype. *J Magn Reson Imaging* 2011; 33:217–220. https://doi.org/10.1002/jmri.22392.

29. Malouf GG, Monzon FA, Couturier J, et al. Genomic heterogeneity of translocation renal cell carcinoma. *Clin Cancer Res* 2013; 19:4673–4684. https://doi.org/10.1158/1078-0432.Ccr-12-3825.

30. Mueller-Peltzer K, de Figueiredo GN, Graf T, Ruebenthaler J, Clevert DA. Papillary renal cell carcinoma in contrast-enhanced ultrasound (CEUS)-a diagnostic performance study. *Clin Hemorheol Microcircul* 2019; 71:159–164. https://doi.org/10.3233/ch-189406.

31. Liu H, Cao H, Chen L, et al. The quantitative evaluation of contrast-enhanced ultrasound in the differentiation of small renal cell carcinoma subtypes and angiomyolipoma. *Quant Imaging Med Surg* 2022; 12:106–118. https://doi.org/10.21037/qims-21-248.

32. Zhang Q, Wei S, Qian X. Conventional ultrasound and contrast-enhanced ultrasound characteristics of different subtypes of

papillary renal cell carcinoma. *Chin J Med Ultrasound (Electron Ed)* 2020; 17:999–1005.

33. Jiang J, Chen Y, Zhou Y, Zhang H. Clear cell renal cell carcinoma: contrast-enhanced ultrasound features relation to tumor size. *Eur J Radiol* 2010; 73:162–167. https://doi.org/10.1016/j.ejrad.2008.09.030.

34. Wang D, Huang X, Bai L, Zhang X, Wei J, Zhou J. Differential diagnosis of chromophobe renal cell carcinoma and papillary renal cell carcinoma with dual-energy spectral computed tomography. *Acta Radiol* 2020; 61:1562–1569. https://doi.org/10.1177/0284185120903447.

35. Raman SP, Johnson PT, Allaf ME, Netto G, Fishman EK. Chromophobe renal cell carcinoma: multiphase MDCT enhancement patterns and morphologic features. *AJR Am J Roentgenol* 2013; 201: 1268–1276. https://doi.org/10.2214/ajr.13.10813.